Eur. Phys. J. D **43**, 201–204 (2007)
DOI: 10.1140/epjd/e2007-00113-x

THE EUROPEAN PHYSICAL JOURNAL D

Dynamical aspects and the role of IVR for the reactivity of noble metal clusters towards molecular oxygen

R. Mitrić, U. Werner, C. Bürgel, and V. Bonačić-Koutecký[a]

Humboldt-Universität zu Berlin, Institut für Chemie, Brook-Taylor-Straße 2, 12489 Berlin, Germany

Received 8 September 2006 / Received in final form 10 October 2006
Published online 24 May 2007 –

Abstract. Here, we present the dynamical aspects and the role of internal energy redistribution (IVR) in the reactivity of noble metal clusters towards O_2. We show on the example of $Ag_3O_2^-$ / Ag_3O_2 / $Ag_3O_2^+$ that NeNePo spectroscopy carried out under zero electron kinetic energy (ZEKE) conditions can be a powerful tool to investigate the geometry relaxation and IVR induced by photodetachment in real time. Furthermore, we demonstrate that difference in the reactivity of Ag_6^- and Au_6^- towards O_2 can be attributed to different nature of the IVR process. Dissipative IVR in Ag_6^- favors fast complex stabilization, whereas resonant IVR found for Au_6^- might be an important factor determining the catalytic activity of Au_6^- cluster in the CO oxidation.

PACS. 31.15.Qg Molecular dynamics and other numerical methods – 31.15.Ar Ab initio calculations

1 Introduction

Noble metal clusters exhibit fascinating reactive properties such as strongly size and charge dependent reactivity towards small molecules such as O_2, CO etc. [1–3]. Moreover, gold clusters have attracted significant attention due to their ability to catalyze the oxidation of CO at low temperatures [4–6]. In this context, the understanding of the mechanism for the activation of molecular oxygen is of fundamental importance. This has stimulated a number of theoretical studies in which specific geometric as well as electronic properties which are responsible for cooperative adsorption of multiple adsorbate molecules on small noble metal clusters, have been identified recently [2,6,7]. In particular, the cooperative effects are regarded essential to the catalytic activity of the gas-phase noble metal clusters in the CO combustion reaction [8,9]. Moreover, since both experimental and theoretical studies have shown that the clusters alone are not capable to break the O–O bond [1,10], the question can be raised whether exploration of reactivity exclusively based on the stationary energetics is sufficient or whether dynamical processes, e.g. internal energy redistribution (IVR) [11], might become the key issue for full understanding of the catalytic properties.

Here, we wish to address two complementary aspects of reaction dynamics of silver and gold clusters towards O_2. One is to study reaction dynamics in neutral clusters in the frame of the negative-to-neutral-to-positive (NeNePo) spectroscopy [12–16]. After an initial ensemble is generated in the anionic electronic ground state, photodetachment of the excess electron occurs and subsequently, dynamics in the neutral state is monitored by probing the cationic state with a laser pulse of sufficiently high energy for ionization. The goal of theoretical fs-NeNePo spectroscopy is to provide conditions under which different processes, such as bond breaking/formation, isomerization and IVR, and their time scales can be observed [17]. The potential prospects of the NeNePo spectroscopy for real time laser spectroscopic investigations of the activation of molecular O_2 will be illustrated on the prototype example of Ag_3O_2.

The second aspect we would like to address concerns differences in reactivity of gold and silver clusters towards O_2 which might be caused by inherently different dynamical properties. It has been found experimentally that $Au_6O_2^-$ is catalyzing the oxidation of CO [18] in contrast to $Ag_6O_2^-$ [19] which is inactive. However, structural and binding properties of $Ag_6O_2^-$ and $Au_6O_2^-$ do not differ substantially. Therefore, the question can be raised whether the pronounced relativistic effects in gold [20–22] might be responsible for the found catalytic activity by invoking a special type of IVR which is reflected in the reaction dynamics and energy redistribution. Therefore, we investigated the differences in the reaction dynamics between silver and gold clusters by studying the collision dynamics of Ag_6^- and Au_6^- with O_2. In particular, we will highlight the role of resonant vs. dissipative IVR in the stabilization of complexes with O_2.

2 Computational

The time-resolved NeNePo spectra were simulated in the framework of our Wigner distribution approach [13] based

[a] e-mail: vbk@chemie.hu-berlin.de

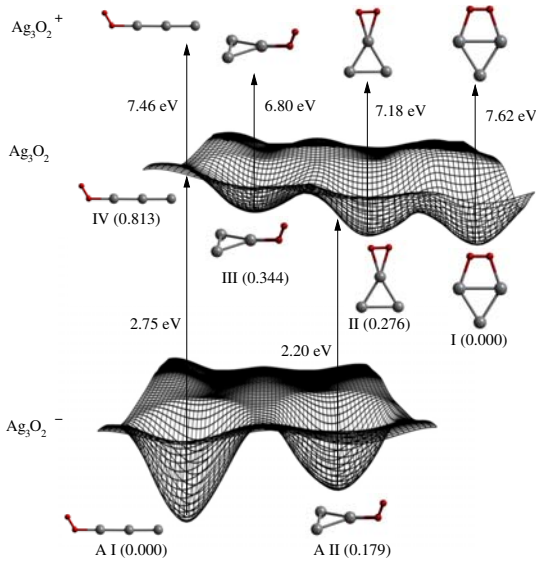

Fig. 1. Scheme of the multistate fs-dynamics for $Ag_3O_2^-/Ag_3O_2/Ag_3O_2^+$ in the framework of NeNePo pump-probe-spectroscopy with structures and energy intervals (in eV) for pump and probe steps.

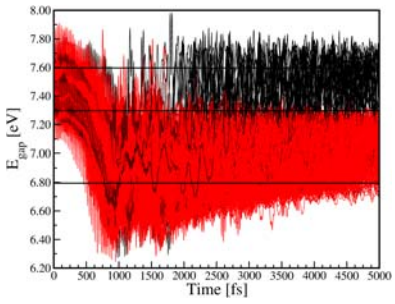

Fig. 2. Bunch of time dependent cation-neutral energy gaps of Ag_3O_2. Trajectories leading to mixture of isomers II and III are marked by light color and trajectories leading to isomer I are marked by black color. Horizontal black lines indicate energies for the probe-pulses at 6.8, 7.3 and 7.6 eV.

on the propagation of an ensemble of classical trajectories carried out "on the fly". Because here the dynamics in the ground electronic states of the neutral species is required, we employ the gradient corrected density functional theory with the atomic orbitals (Gaussian basis sets). For details on electronic structure calculations, cf. reference [17]. The collision dynamics of Ag_6^- and Au_6^- with O_2 has been investigated employing DFT methods with the gradient corrected PBE functional [23] using Stuttgart $19e^-$ RECP [24] for Ag and Au and triple zeta polarization basis set for O [25]. The collision parameters have been sampled resulting in ≈400 initial conditions. Collisional impact energy of 0.25 eV has been chosen corresponding to room temperature.

3 Results and discussion

Simulation of NeNePo spectra for $Ag_3O_2^-$ / Ag_3O_2 / $Ag_3O_2^+$

The electronic and structural aspects of adsorption of molecular oxygen on anionic silver clusters have been investigated previously [7]. Here, we present the simulation of the NeNePo spectra of $Ag_3O_2^-$ / Ag_3O_2 / $Ag_3O_2^+$ [16] with the specific goal to address the energy redistribution process which occurs upon geometry relaxation induced by the photodetachment process.

In Figure 1, the scheme for the multistate dynamics of the $Ag_3O_2^-$ / Ag_3O_2 / $Ag_3O_2^+$ system is shown. In the anionic state, two isomers with linear (A I) and triangular (A II) Ag_3 subunit are very close in energy (0.179 eV). The exact energy sequence is very difficult to determine, even with highly accurate methods. On the other hand, the difference in the vertical detachment energies (VDE) between the two isomers (2.8 eV for isomer A I and 2.2 eV for isomer A II) allows for selective excitation of only one isomer by choice of the appropriate pump-pulse energy. Therefore, in the simulations presented here we assume that only the linear isomer A I is populated. A canonical Wigner distribution function is used to generate the initial conditions at $T = 20$ K.

After photodetachment with a pump-pulse energy of 2.75 eV, a transition state on the neutral PES of Ag_3O_2 is reached. As shown in Figure 1, three isomers are present in the neutral state which mainly differ in the binding situation of the O_2 subunit. In the global minimum (I) oxygen bridges two silver atoms, whereas in the two higher lying isomers oxygen is bound to one silver atom, forming two (II) or one bond (III), respectively (cf. Fig. 1).

The dynamics in the neutral state induced by the photodetachment is dominated by relaxation of the Ag_3 subunit from the linear to the triangular form. This process is completed within 1 ps, as can be seen from the time dependent energy gaps between the neutral and the cationic state presented in Figure 2 (light lines). Subsequently, the energy gained during this process is partially transferred to the molecular oxygen, leading to a mixture of neutral isomers II and III. At later times, two different isomerization pathways can be identified from Figure 2. A mixture of the two neutral isomers II and III with higher energies still remains dominant channel (light lines, 90%) while the channel leading to the global minimum (I) amounts only to about 10% of the population within the simulation period of 5 ps (cf. black curves in Fig. 2).

The simulated signal under zero electron kinetic energy condition (NeNePo-ZEKE) and including continuum (NeNePo) for three different probe-pulse energies 6.8, 7.3 and 7.6 eV (cf. horizontal lines in Fig. 2) are presented in Figure 3. For the probe-pulse energy of 6.8 eV, the NeNePo-ZEKE signal reflects the main isomerization process into a mixture of the two higher lying neutral isomers due to close lying values of the ionization potentials of 6.8 eV (isomer III) and 7.18 eV (isomer II). Since the contribution of the continuum for the 6.8 eV probe-pulse energy is very small, there is no significant difference between the NeNePo and NeNePo-ZEKE signals.

Under ZEKE conditions, the probe-pulse energy of 7.3 eV allows monitoring the onset of the relaxation dynamics of the Ag_3 subunit at ≈500 fs. However, if the

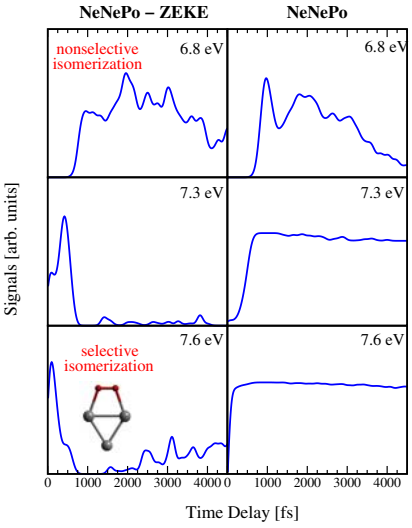

Fig. 3. Simulated NeNePo-ZEKE and NeNePo signals of Ag_3O_2 for 20 K initial condition ensemble at probe-energies 6.8, 7.3 and 7.6 eV.

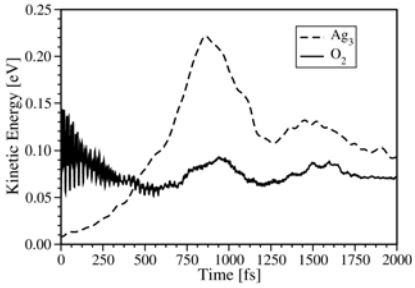

Fig. 4. Distribution of the kinetic energy between Ag_3 and O_2 fragment.

continuum is included the signal increases for 800 fs and then remains constant which means that relaxation dynamics is smeared out. The ZEKE signal with a probe-pulse energy of 7.6 eV exhibits a fast decay within 1 ps due to the escape from the Franck-Condon region, which is initially populated after the photodetachment. Moreover, after 1.5 ps the signal starts to rise again indicating the increasing population of the global minimum (IP = 7.62 eV). This signal offers the opportunity to identify isomerization processes leading to the global minimum. The global minimum starts to be populated at 1.5 ps and the population reaches ≈10% after 4 ps. On the contrary, the NeNePo signal for the same energy does not allow to distinguish any processes due to the fact that all structures are ionized.

In order to study the IVR process initiated by the photodetachment we present in Figure 4 the distribution of the kinetic energy between the Ag_3 and the O_2 fragments. The oscillations of the kinetic energy of O_2 within the first 700 fs reflects the thermally excited vibrations of the molecular oxygen. For the Ag_3 subunit, the kinetic energy starts to rise due to relaxation processes up to a maximum at 850 fs, which corresponds to the time of the closest approach of both silver atoms (internal collision). The timescale for this relaxation process is quite similar to those of the free Ag_3 [13], in which internal collision occurs after 950 fs. Subsequently, the increasing distance of the silver atoms after the collision results in a decay of the kinetic energy up to a minimum at 1270 fs. The parallel increase of the O_2 kinetic energy with a maximum at 950 fs indicates partial energy transfer from the Ag_3 to the O_2 fragment. A second maximum of the Ag_3 kinetic energy at 1450 fs can be assigned to the second collision of the silver atoms, also followed by a partial energy transfer to the oxygen fragment.

The resulting increase of kinetic energy in the O_2 fragment leads to the two different isomerization pathways described above. The kinetic energy in the oxygen fragment is not sufficient to overcome the energy barrier for the isomerization into the global minimum. Therefore, only about 10% of the ensemble is able to reach the global minimum within the simulated time interval. The most efficient isomerization occurs between isomer II and III.

Collisions of Ag_6^- and Au_6^- with O_2

In order to address the influence of the dynamics and in particular the IVR process on the reaction between Ag_6^- and Au_6^- with molecular O_2, we compared the reaction dynamics by simulating collisions between clusters and O_2. In particular, the question, whether different reaction dynamics caused by the relativistic effects which are more pronounced for gold than for silver might be responsible for the observed different catalytic activity will be addressed.

As can be seen from Figure 5, in the case of $Ag_6^- + O_2$, dissipative IVR from O_2 to cluster can be identified. The kinetic energy of the complex is mainly localized in the Ag_6 subunit (black curve in Fig. 5a) after the first 1.4 ps. This efficient process leads to fast stabilization of the complex and furthermore, prevents activation of O_2. Moreover, due to excess of adsorption energy, a large deviation from planarity is observed as can be seen from the snapshots of the MD trajectory (inset in Fig. 5a). In contrast, in the case of $Au_6^- + O_2$ a resonant IVR is present which can be seen from Figure 5b. The kinetic energy is periodically distributed over both Au_6 and O_2 subgroups for a longer period of time allowing O_2 to remain activated for longer times. In contrast to Ag_6^-, no large deviation from planarity has been identified. Consequently, in the case of gold clusters the adsorption energy remains localized at the adsorption site and therefore might be used to more easily overcome reaction barriers.

Notice that the differences in energy redistribution are not caused by different masses but are present due to inherent different dynamical processes connected with higher rigidity of Au_6^- caused by pronounced relativistic effects. This leads to more directional bonding in Au_6^- due to the increased contribution of *d*-electrons [21,26]. This directionality is also reflected in more rigid structure of Au_6^-. In contrast, the *s*-like delocalized bonding in Ag_6^- gives rise to flat energy surface with close lying isomers.

In order to prove the higher rigidity of Au_6^-, MD simulations of the isomerization dynamics of Ag_6^- and Au_6^- have been performed at different temperatures (cf. Fig. 5c). We use Lindemann index δ as a measure of rigidity. At similar temperatures δ has much higher values for silver than for gold indicating higher rigidity of Au_6^-. Clearly, the Lindemann index δ reaches higher values at

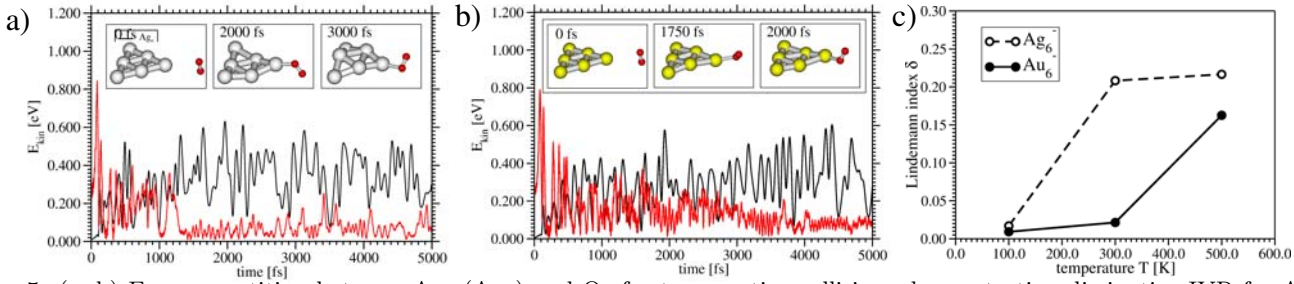

Fig. 5. (a, b) Energy partition between Ag_6 (Au_6) and O_2 for two reactive collisions demonstrating dissipative IVR for Ag_6^- (a) and resonant IVR for Au_6^- (b). For illustration, representative single trajectory has been chosen. Red: $E_{kin}(O_2)$; black: $E_{kin}(Ag_6/Au_6)$. (c) Lindemann indices δ for Ag_6^- (dashed line) and Au_6^- (solid line) at different temperatures.

lower temperature for silver compared to gold indicating melting at lower temperature in the former case.

In summary, we have shown that the energy redistribution process is much more efficient in the case of Ag_6^- than for Au_6^-. This leads to the fast stabilization of the complex with O_2. In contrast to that, upon collision of Au_6^- with O_2 resonant IVR process occurs which might facilitate the overcoming of the barriers in subsequent reactions with CO. Thus we have shown that dynamical aspects might significantly influence the reactivity properties of clusters and can be an important factor which determines potential catalytic activity.

4 Conclusion

We have presented two complementary theoretical investigations which allowed us to study the energy redistribution in neutral and anionic complexes between noble metal clusters and molecular oxygen. We have shown that geometric relaxation and IVR process can be identified in real time in the framework of the NeNePo spectroscopy. Our theoretical simulation predicts, that it is mandatory to carry out experiments close to ZEKE condition in order to distinguish different processes in the NeNePo spectra. Furthermore, we have demonstrated that different IVR processes can significantly influence the reactivity of anionic gold and silver clusters towards O_2. By studying collisional dynamics of Ag_6^- and Au_6^- with O_2 we have shown that differences in their reactivity can be attributed to different nature of the IVR process. Fast dissipative IVR in Ag_6^- is favorable for the complex stabilization leading to a complex which is not catalytically active. In contrast, the resonant IVR process in Au_6^- gives rise to an energy localization at the active site which might facilitate O–O bond breaking in the reaction with CO.

This work was supported by the Deutsche Forschungsgemeinschaft SFB 450.

References

1. T.H. Lee, K.M. Ervin, J. Phys. Chem. **98**, 10023 (1994)
2. W.T. Wallace, R.B. Wyrwas, R.L. Whetten, R. Mitrić, V. Bonačić-Koutecký, J. Am. Chem. Soc. **125**, 8408 (2003)
3. T.M. Bernhardt, Int. J. Mass. Spectrom. **243**, 1 (2005)
4. M. Haruta, Catal. Today **36**, 153 (1997)
5. A. Sanchez, S. Abbet, U. Heiz, W.D. Schneider, H. Häkkinen, R.N. Barnett, U. Landman, J. Phys. Chem. A **103**, 9573 (1999)
6. B. Yoon, H. Häkkinen, U. Landman, J. Phys. Chem. A **107**, 4066 (2003)
7. J. Hagen, L.D. Socaciu, J. Le Roux, D. Popolan, T.M. Bernhardt, L. Wöste, R. Mitrić, V. Bonačić-Koutecký, J. Am. Chem. Soc. **126**, 3442 (2004)
8. M.L. Kimble, A.W. Castleman Jr, R. Mitrić, C. Bürgel, V. Bonačić-Koutecký, J. Am. Chem. Soc. **126**, 2526 (2004)
9. V. Bonačić-Koutecký, R. Mitrić, C. Bürgel, H. Noack, M. Hartmann, J. Pittner, Eur. Phys. J. D **34**, 113 (2005)
10. D. Stolčić, M. Fischer, G. Ganteför, Y.D. Kim, Q. Sun, P. Jena, J. Am. Chem. Soc. **125**, 2848 (2003)
11. K.F. Freed, J. Jortner, J. Chem. Phys. **52**, 6272 (1970)
12. S. Wolf, G. Sommerer, S. Rutz, E. Schreiber, T. Leisner, L. Wöste, R.S. Berry, Phys. Rev. Lett. **74**, 4177 (1995)
13. M. Hartmann, J. Pittner, V. Bonačić-Koutecký, A. Heidenreich, J. Jortner, J. Chem. Phys. **108**, 3096 (1998)
14. R. Mitrić, M. Hartmann, B. Stanca, V. Bonačić-Koutecký, P. Fantucci, J. Phys. Chem. A **105**, 8892 (2001)
15. T.M. Bernhardt, J. Hagen, L.D. Socaciu, J. Le Roux, D. Popolan, M. Vaida, L. Wöste, R. Mitrić, V. Bonačić-Koutecký, A. Heidenreich, J. Jortner, Chem. Phys. Chem. **6**, 243 (2005)
16. V. Bonačić-Koutecký, R. Mitrić, U. Werner, L. Wöste, R.S. Berry, Proc. Nat. Acad. Sci. **103**, 10594 (2006)
17. V. Bonačić-Koutecký, R. Mitrić, Chem. Rev. **105**, 11 (2005)
18. W.T. Wallace, R.L. Whetten, J. Am. Chem. Soc. **124**, 7499 (2002)
19. L.D. Socaciu, J. Hagen, J. Le Roux, D. Popolan, T.M. Bernhardt, L. Wöste, S. Vajda, Chem. Phys. **120**, 2078 (2004)
20. H. Häkkinen, M. Moseler, U. Landman, Phys. Rev. Lett. **89**, 033401 (2002)
21. V. Bonačić-Koutecký, J. Burda, M. Ge, R. Mitrić, G. Zampella, R. Fantucci, J. Chem. Phys. **117**, 3120 (2002)
22. F. Furche, R. Ahlrichs, P. Weis, C. Jacob, S. Gilb, T. Bierweiler, M.M. Kappes, J. Chem. Phys. **117**, 6982 (2002)
23. J.P. Perdew, K. Burke, M. Ernzerhof, Phys. Rev. Lett. **77**, 3865 (1996)
24. D. Andrae, U. Haeussermann, M. Dolg, H. Stoll, H. Preuss, Theor. Chim. Acta **77**, 123 (1990)
25. A. Schäfer, C. Huber, R. Ahlrichs, J. Chem. Phys. **100**, 5829 (1994)
26. R. Mitrić, C. Bürgel, J. Burda, V. Bonačić-Koutecký, Eur. Phys. J. D **24**, 41 (2003)